Interacting multiple model-based human motion prediction for motion planning of companion robots

Donghan Lee[1], Chang Liu[2] and J. Karl Hedrick[3]

***Abstract*— Motion planning of human-companion robots is a challenging problem and its solution has numerous applications. This paper proposes an autonomous motion planning framework for human-companion robots to accompany humans in a socially desirable manner, which takes into account the safety and comfort requirements. An Interacting Multiple Model-Unscented Kalman Filter (IMM-UKF) estimation and prediction approach is developed to estimate human motion states from sensor data and predict human position and speed for a finite horizon. Based on the predicted human states, the robot motion planning is formulated as a model predictive control (MPC) problem. Simulations have demonstrated the superior performance of the IMM-UKF approach and the effectiveness of the MPC planner in facilitating the socially desirable companion behavior.**

I. INTRODUCTION

The application of autonomous robots for search-and-rescue (SAR) missions have received considerable attentions in last decades [1]–[3]. One particular interesting scenario is allowing robots to autonomously accompany human rescuers during the SAR, assisting in carrying heavy apparatus, detecting signals of survivors or exploring dangerous areas.

To make the robot's companion behavior natural and amiable, referred to as *socially desirable*, several requirements need to be satisfied, including the safety and comfort [4]. Safety serves as the fundamental guideline, requiring that robots avoid collision with accompanied humans under all circumstances [5]. Comfort requires robots to pose little annoyance and stress for the accompanied humans [4], which is mainly formulated regarding the distance that a robot needs to keep from people. The "Proxemics" model, proposed by Hall et al. [6], has been adopted for designing robot's human-friendly motion behavior [7]. This model denotes a virtual zone around a person that robots should avoiding entering to prevent the discomfort that the person may feel. Similarity on speed between the human and the robot has also been considered as a contributing factor for comfort [8].

In order to generate socially desirable motion behavior, accurate human motion prediction is necessary. To be specific, a robot needs to predict human future trajectory based on human's motion states that are obtained from measurement tools such as GPS sensors or cameras. Filtering methods, such as Kalman filters (KF) and particle filters (PF), have been applied for tracking moving objects [9], [10], assuming certain motion pattern, such as constant speed and direction [5]. These single-model filtering approaches can effectively predict human motion when people follow a pre-determined motion pattern. However, when the human movement involves multiple models, such as making turns with changing speed, such methods may fail to give accurate prediction.

Learning techniques have also been utilized for human motion prediction in recent years. Bennewitz et al. [11] proposed a prediction approach based on the hidden Markov model, utilizing the clustered collections of trajectories that characterize typical motion patterns of persons. Fulgenzi et al. [12] developed a Gaussian process-based motion predictor, using pre-learned human motion patterns. These learning-based approaches have achieved success in predicting human motion in the environments where human trajectories have been previously collected for training. However, they may fail to obtain accurate prediction in unknown environments that no training data is available. This drawback renders the learning-based prediction methods less applicable for SAR missions since disaster sites are diverse and rarely similar to the known ones.

In this work, we propose an Interacting Multiple Model (IMM)-based human motion estimation and prediction approach, taking advantage of the fact that human motion usually involves different motion models [13], such as straight-line movement, making turns and change of speed. The IMM-based approach incorporates several motion models and dynamically adjusts the mode probabilities based on the observed human trajectory. To deal with the nonlinearity of the human motion, such as making turns, Unscented Kalman Filter(UKF) is applied to each model in the IMM framework, resulting in the so-called IMM-UKF approach. Such approach can achieve higher prediction accuracy and faster response compared to single-model filtering methods such as KF and PF. Additionally, IMM-UKF does not need training and is thus applicable to unknown environments, which is advantageous over learning-based methods for SAR missions.

Utilizing the predicted human trajectory, a model predictive control (MPC)-based motion planner is developed that formulates the motion planning as a nonlinear programming, which conveniently considers the safety and comfort requirements. The MPC planner with IMM-UKF prediction is evaluated using a simulated SAR scenario, in which the human rescuer moves sequentially to several destinations

[1]Donghan Lee is with the Vehicle Dynamics & Control Lab, Department of Mechanical Engineering, University of California at Berkeley, California 94720, USA donghan.lee@berkeley.edu

[2]Chang Liu is with the Vehicle Dynamics & Control Lab, Department of Mechanical Engineering, University of California at Berkeley, California 94720, USA changliu@berkeley.edu

[3]J. Karl Hedrick is with Faculty of Mechanical Engineering, University of California at Berkeley, California 94720, USA khedrick@berkeley.edu

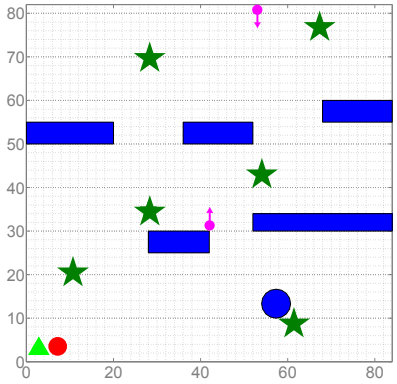

Fig. 1: A search-and-rescue scenario for the companion robot to accompany a human. The red circle and the green triangle represent the human rescuer and the robot companion, respectively.

and the robot needs to accompany. Simulation results show that the IMM-UKF provides superior prediction performance than other methods. Using the MPC motion planner, the robot has successfully accompanied the human in a safe and comfortable manner.

The remainder of this paper is organized as follows: The problem of motion planning for a human-companion robot is formulated for the SAR mission in Section II. Section III proposes the IMM-UKF human state estimation and prediction method, followed by description of the MPC-based motion planner. Simulation setup and results on evaluating the proposed approach are presented in Section IV. Section V concludes the paper with ideas of future work.

II. PROBLEM FORMULATION

Consider a SAR scenario (Fig. 1) in which a human first responder needs to deliver medical treatment to several destinations that contain injured people. The environmental information, such as position and dimension of obstacles, can be provided by using satellite maps or aerial images. A companion robot that carries medical apparatus will accompany the human and sequentially move to these destinations. The robot has no knowledge about the positions of human destinations. However, it can measure human positions in real time from the measurement tools such as GPS sensors or cameras.

Several obstacles exist in the field, including five stationary ones (blue rectangles), representing unmovable obstructions such as buildings or plants, and two moving ones (pink dots with arrows showing moving direction) representing mobile objects such as pedestrians or vehicles. The positions of stationary obstacles are known to both the human and the companion robot while the moving obstacles are measured using same measurement tool for tracking the human rescuer. When accompanying the human, the robot should satisfy the aforementioned safety and comfort requirements, illustrated in Fig. 2. To be specific, a circular "unsafety zone" (blue circle) with radius d_s is defined around the target person. Stepping into the "unsafety zone" is considered as unsafe

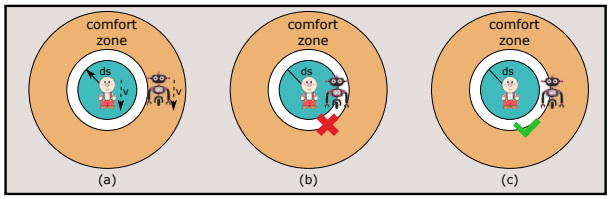

Fig. 2: Illustration of safety and comfort requirements. (a) The most desirable companion behavior is that the robot stays within the "comfort range" and maintains similar speed as the human. (b) The robot is not allowed to enter the "unsafety zone". (c) It is acceptable, but not desirable, that the robot stays outside of the "comfort range" and the "unsafety zone".

behavior and thus should be strictly prohibited. The comfort requires the robot to stay within a "comfort range" (orange area) of distance from the human and also keep similar speed. Comfort is a soft constraint in that it is acceptable, but not desirable, that the robot moves outside of the "comfort range".

III. METHODS

A. Human Motion Estimation and Prediction

1) Interacting Multiple Model: The Interacting Multiple Model (IMM) approach are usually applied for estimating the system states from the noisy sensor data. It utilizes a bank of r number of filters, each corresponding to a different motion model. State estimate at time k is computed as a weighted sum of estimates from each filter, as shown in the following formula:

$$\hat{x}(k|k) = \sum_{j=1}^{r} \mu_j(k)\hat{x}^j(k|k) \tag{1}$$

where $\hat{x}^j(k|k)$ represents the state estimate from the j^{th} filter; $\mu_j(k)$ stands for the mode probability and is computed as follows:

$$\mu_j(k) = \frac{1}{c}\sum_{i=1}^{r} L_{ij}(k)p_{ij}\mu_j(k-1)$$

where c denotes the normalizing factor; $L_{ij}(k)$ stands for the Gaussian likelihood of receiving the current measurement given all previous measurements and that the j^{th} model is in effect at time k; p_{ij} represents the mode transition probability from the i^{th} to the j^{th} model. Each filter uses the mixed initial state estimate and covariance from an interaction of the r filters, which consists of the combination of the estimates with the mixing probability at previous time step. Readers interested in the details of the IMM approach can refer to [14].

In this work, two different kinematic models are used in the IMM framework: one is the coordinated turn motion model, reflecting the action of making turns or moving along a curved path, and the other is the uniform motion model, representing the straight-line movement. The equation for the

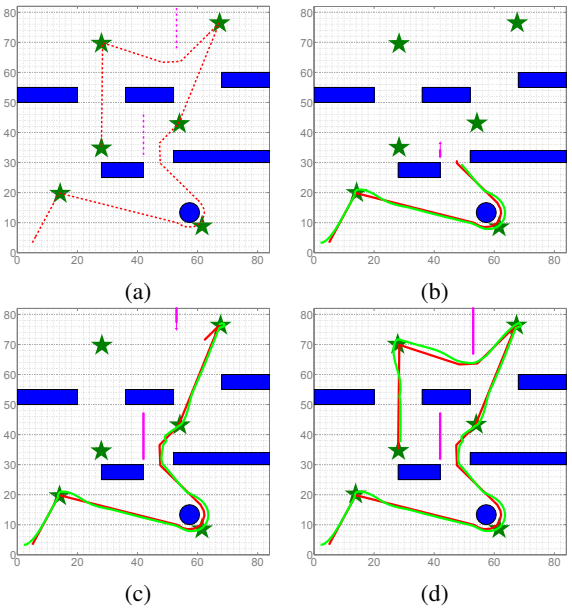

Fig. 3: A screenshot of the simulation. The red line represents the human trajectory and the green one shows the companion robot's trajectory.

coordinated turn motion is shown below:

$$x^{h,1}(k+1) = f(x^{h,1}(k)) + Gw_1(k)$$

$$f(x^{h,1}(k)) = \begin{bmatrix} p_1^h + \frac{\sin(\omega^h T)}{\omega^h} v_1^h - \frac{1-\cos(\omega^h T)}{\omega^h} v_2^h \\ \cos(\omega^h T) v_1^h - \sin(\omega^h T) v_2^h \\ p_2^h + \frac{1-\cos(\omega^h T)}{\omega^h} v_1^h + \frac{\sin(\omega^h T)}{\omega^h} v_2^h \\ \sin(\omega^h T) v_1^h + \cos(\omega^h T) v_2^h \\ \omega^h \end{bmatrix}$$

$$G = \begin{bmatrix} \frac{T^2}{2} & 0 & 0 \\ T & 0 & 0 \\ 0 & \frac{T^2}{2} & 0 \\ 0 & T & 0 \\ 0 & 0 & 1 \end{bmatrix}$$

$$w_1 \sim \mathcal{N}(0, Q).$$

Also, the equation of the uniform motion is represented as follows:

$$x^{h,2}(k+1) = Ax^{h,2}(k) + Bw_2(k)$$

$$A = \begin{bmatrix} 1 & T & 0 & 0 & 0 \\ 0 & 1 & 0 & 0 & 0 \\ 0 & 0 & 1 & T & 0 \\ 0 & 0 & 0 & 1 & 0 \\ 0 & 0 & 0 & 0 & 0 \end{bmatrix}, \; B = \begin{bmatrix} \frac{T^2}{2} & 0 & 0 \\ T & 0 & 0 \\ 0 & \frac{T^2}{2} & 0 \\ 0 & T & 0 \\ 0 & 0 & 1 \end{bmatrix}$$

$$w_2 \sim \mathcal{N}(0, Q)$$

where $x^{h,i}(k)$, $i = 1, 2$ represents the human motion state including five elements : $p_1^h, v_1^h, p_2^h, v_2^h, \omega^h$, where p_1^h, p_2^h denote the longitudinal and lateral position of the human, v_1^h, v_2^h the corresponding velocity and ω^h the turn rate of the human; $w_i(k)$, $i = 1, 2$ represents process noise; T represents the sampling time; Q is the covariance matrix of the process noise.

The uniform motion model is essentially a special case of the coordinated turn motion model with the turn rate ω being fixed to zero. It seems that only considering the coordinated turn motion model suffices to estimate human motion states, in addition to the benefits of reduced computations by using the single model. However, including two models are necessary since this allows the estimator for fast detection of change of motions, which is shown in [15]. The ability to quickly detect the change of the motion is one of the important properties for the estimation and prediction.

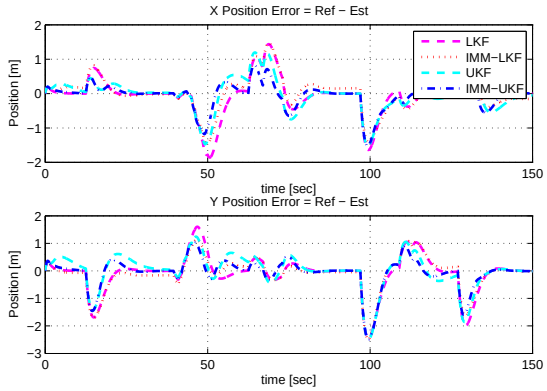

Fig. 4: Comparison of position estimation error with LKF, IMM-LKF, UKF and IMM-UKF

The observation equation is represented as :

$$y^h(k) = Cx^h(k) + v(k) \tag{2}$$

where $y^h(k)$ denotes the observed human state at the time step k; $v(k)$ stands for measurement noise.

By using GPS sensors, the human positions can be measured. Therefore, the parameters in observation model Eq. (2) is defined as:

$$C = \begin{bmatrix} 1 & 0 & 0 & 0 \\ 0 & 0 & 1 & 0 \end{bmatrix}, v \sim \mathcal{N}(0, V)$$

where V is the convariance matrix of the measurement noise. The above two models are utilized for human motion state estimation, in combination with the Unscented Kalman Filter.

2) Unscented Kalman Filter: The Unscented Kalman Filter (UKF) is applied to each model that are used in IMM framework for estimating human states. It is an effective state estimation technique for nonlinear systems by implementing the Unscented Transformation (UT) that calculates the statistics of a random vector that undergoes a nonlinear transformation [16]. To be specific, given an arbitrary nonlinear motion model $z = g(x)$ and a L-dimensional Gaussian Random Vector (GRV) x with mean $\hat{x}$ and covariance P_x, the statistics of z can be approximated by using $2L+1$ discrete sample points $\{\chi^{(i)}\}_{i=0}^{2L} = \{\hat{x} \text{ and } \hat{x} \pm \sigma_j, j = 1, ..., L\}$, called *sigma points*, where σ_j is the j^{th} column of the matrix $\sqrt{(L+\lambda)P_x}$. λ is a scaling parameter, as defined below:

$$\lambda = \alpha^2(L + \kappa) - L \tag{3a}$$

$$W_0^{(m)} = \frac{\lambda}{L+\lambda} \tag{3b}$$

$$W_0^{(c)} = \frac{\lambda}{L+\lambda} + 1 - \alpha^2 + \beta \tag{3c}$$

$$W_i^{(m)} = W_i^{(c)} = \frac{1}{L+\lambda}, \quad i = 1, ..., 2L \tag{3d}$$

where α determines the spread of sigma points about the mean $\hat{x}$; κ is a secondary scaling parameter; β is used to incorporate prior knowledge of the distribution.

Once the sigma points have been generated, each point is passed through the nonlinear function $z = g(x)$, i.e. each column of the sigma points is propagated through the nonlinearity, as in $\zeta^{(i)} = g(\chi^{(i)}), i = 0, ..., 2L$. The mean $\hat{z}$ and the covariance P_z are approximated as $\hat{z} \simeq \Sigma_{i=0}^{2L} W_i^{(m)} \zeta^{(i)}$ and $P_z \simeq \Sigma_{i=0}^{2L} W_i^{(c)} (\zeta^{(i)} - \hat{z})(\zeta^{(i)} - \hat{z})^{\mathsf{T}}$, calculated as given in above equations of the weights and parameters [17]. The state estimate, $\hat{x}^j(k|k)$, $j = 1, ..., r$ in Eq. (1), can be computed like $\hat{z}$ at each filter that corresponds to a different motion model. Readers can refer to [16] for more details of the UKF algorithm.

3) Human Motion Prediction: The IMM approach is extended to predict human motion in this paper. The estimated human motion states and the mode probabilities are utilized for predicting human future states. To be specific, using the uniform motion model and the turn motion model, human positions for each model can be extrapolated and then combined based on the mode probabilities to obtain the predicted positions. Let $\hat{x}^{h,j}(k|k)$ and $\tilde{x}^{h,j}(k+i|k)$ represent the estimated and predicted human states associated with the j^{th} model at time k and $k+i\,(i \geq 0)$, respectively, based on the observations up to time k. The prediction procedure works as follows:

$$\tilde{x}^h(k+l+1|k) = \sum_{j=1}^{r} \mu_j \tilde{x}^{h,j}(k+l+1|k), l = 0, \ldots, N-1 \tag{4a}$$

$$\tilde{x}^{h,j}(k+l+1|k) = \Sigma_{i=0}^{2L} W_i^{(m)} \chi_{k+l+1|k}^{(i)}, j = 1, \ldots, r \tag{4b}$$

$$\chi_{k+l+1|k}^{(i)} = f(\chi_{k+l|k}^{(i)}) \quad i = 0, \ldots, 2L \tag{4c}$$

$$\chi_{k|k}^{(i)} = \left[\hat{x}^{h,j}(k|k),\ \hat{x}^{h,j}(k|k) \pm \sigma_m^{h,j}(k|k)\right] \tag{4d}$$
$$m = 1, \ldots, L$$

where N denotes the prediction horizon; L is the dimension of $x^{h,j}$; $\sigma_m^{h,j}(k|k)$ is the m^{th} column of the matrix $\sqrt{(L+\lambda)P_x^{h,j}(k|k)}$; $P_x^{h,j}(k|k)$ stands for the covariance associated with the j^{th} model at time k; λ is represented in Eq. (3a).

B. Robot motion Planning

The model predictive control (MPC) approach is utilized for robot motion planning. It iteratively solves a finite-horizon constrained optimal control problem: after computing the optimal control inputs over the planning horizon, it implements the first input and then computes for a new set of control inputs, starting from the updated state. Let $p^h(k) = \begin{bmatrix} p_1^h(k) \\ p_2^h(k) \end{bmatrix}$ and $v^h(k) = \left\| \begin{bmatrix} v_1^h(k) \\ v_2^h(k) \end{bmatrix} \right\|_2$ represent the position vector and the speed of the human at time k, respectively. Notations for the estimated and predicted position vector and speed can be defined as $\hat{p}^h(k|k), \tilde{p}^h(k+i|k), \hat{v}^h(k|k), \tilde{v}^h(k+i|k)$, respectively. The optimal control inputs are obtained by solving the following nonlinear programming problem that incorporates the dynamics of the robot and the safety and comfort requirements:

$$\min_{\mathbf{A}_k, \mathbf{\Theta}_k} \quad \sum_{i=1}^{N} q_1 \left| \left\| \bar{p}^r(k+i|k) - \tilde{p}^h(k+i|k) \right\|_2^2 - d_c^2 \right| + q_2 \left| \bar{v}^r(k+i|k) - \tilde{v}^h(k+i|k) \right|^2 \tag{5a}$$

$$\text{s.t.} \quad \bar{p}^r(k+i|k) = \bar{p}^r(k+i-1|k) + \bar{v}^r(k+i-1|k) \begin{bmatrix} \cos\theta(k) \\ \sin\theta(k) \end{bmatrix} T \tag{5b}$$

$$\bar{v}^r(k+i|k) = \bar{v}^r(k+i-1|k) + \bar{a}^r(k+i-1|k)T \tag{5c}$$

$$\bar{\theta}^r(k+i|k) = \bar{\theta}^r(k+i-1|k) + \bar{\omega}(k+i-1|k)T \tag{5d}$$

$$a_{lb} \leq \bar{a}^r(k) \leq a_{ub},\ w_{lb} \leq \bar{\omega}^r(k) \leq w_{ub} \tag{5e}$$

$$||\bar{p}^r(k+i|k) - \tilde{p}^h(k+i|k)||_2 > d_s \tag{5f}$$

$$||\bar{p}^r(k+i|k) - \tilde{p}_{l_m}^{obs_m}(k+i|k)||_2 > d_s \tag{5g}$$
$$l_m = 1, \ldots, n_m$$

$$h_{l_s}(\bar{p}^r(k+i|k)) > 0 \tag{5h}$$

$$h_{l_s}(\lambda \bar{p}^r(k+i-1|k) + (1-\lambda)\bar{p}^r(k+i|k)) > 0 \tag{5i}$$
$$l_s = 1, \ldots, n_s,\ \forall \lambda \in [0,1]$$

$$\bar{p}^r(k|k) = p^r(k), \bar{v}^r(k|k) = v^r(k), \bar{\theta}^r(k|k) = \theta^r(k) \tag{5j}$$

where $\bar{p}^r(k+i|k)$, $\bar{v}^r(k+i|k)$ and $\bar{\theta}(k+i|k)$, $1 \leq i \leq N$ represent the planned position, speed and heading angle of the robot at time $k+i$, respectively; n_m stands for the number of moving obstacles and $\tilde{p}_{l_m}^{obs_m}$ denotes the predicted position of the l_m-th moving obstacle; n_s is the number of static obstacles. The static obstacles are approximated by ellipses, the details of which are described in the Appendix-B. $h_{l_s}(\cdot)$ denotes the analytical function of the ellipse approximation of the l_s-th static obstacle. $(\mathbf{A}_k, \mathbf{\Theta}_k)$ stand for the set of optimal acceleration $\bar{a}^r$ and angular velocity $\bar{\omega}^r$ of the robot in the prediction horizon $[k, k+N-1]$, obtained by solving the above optimization problem at time k. $\bar{a}^r(k)$ and $\bar{\omega}^r(k)$ are implemented as the robot's control input at time k.

The objective function Eq. (5a) consists of two terms: the first one stands for the difference between the squared human-robot distances and the squared comfort distance d_c that takes the intermediate value of the "comfort range"; the second one represents the speed difference between the robot and the human. This reflects the comfort requirement that the robot stay within the "comfort range" from the human and keep similar pace at the same time. q_1 and q_2 denote the weights for these two terms.

The robot dynamics are defined in Eqs. (5b) to (5d) with Eq. (5e) being the bounds on control inputs. The safety constraints are imposed in Eqs. (5f) to (5i). Eqs. (5f) and (5g) regulates that the robot stay at least the safety distance d_s from the human and moving obstacles in order to avoid collision. To predict the position of moving obstacles, the same motion prediction method described in Section III-A.3 is applied. Eqs. (5h) and (5i) enforce the collision avoidance with static obstacles. To be specific, Eq. (5h) demands that each way point of the robot be kept outside of static obstacles and Eq. (5i) requires that the trajectory connecting the adjacent waypoints not intersect with obstacles, which

eliminates the path that leads the robot across obstacles. Eq. (5j) initializes the robot's planned states based on its actual state at time k.

IV. SIMULATION RESULTS & DISCUSSION

A. Simulation setup

Simulations have been run to evaluate the proposed MPC planner with IMM-UKF for prediction. A human rescuer will move sequentially to six targets with constant speed of $1.5m/s$ which is the normal walking speed of human in a $84m \times 82m$ field, following the trajectory as shown in Fig. 3a. Notice that such trajectory covers several typical human motion patterns, including straight-line movement, motion following curved paths and making sharp turns. Therefore, it provides a realistic testbed for evaluating the proposed MPC planner with IMM-UKF for prediction. Both the trajectory and human speed are unrevealed to the robot. The safety distance d_s is chosen as $1m$. According to the research by Hall et al. [6], the comfort distance range is from $1.2m$ to $3.6m$. In the simulation, d_c is chosen as $2.4m$. Any distance within $[1.2m, 3.6m]$ is considered a comfortable one, but the closer distance to $2.4m$ is more preferable. The sampling rate of GPS sensor is $20Hz$ and the variance of sensor measurement noise is considered as $0.5m$. The robot's maximum acceleration and deceleration are set to be $1m/s^2$ and $-3m/s^2$ respectively and the angular velocity range is chosen to be $[-90°/s, 90°/s]$. In the IMM estimator, the process noise and the measurement noise are set to be 1.5×10^{-2} and 1.5, respectively. The parameters of UKF in the estimator are $L = 5, \alpha = 0.001, \kappa = 0$ and $\beta = 2$. The prediction horizon for the human motion is chosen as $2.5s$ and the robot iteratively computes the control inputs every $500ms$.

B. Simulation results

Figs. 3a to 3d show both the human and robot's trajectories. The performance of human motion estimation and prediction is evaluated by comparing with three other filtering methods. The MPC-based robot motion planning method is then evaluated under different prediction strategies.

1) Human motion estimation: The error between the estimated and the actual human position and speed at each time step are compared to evaluate the estimation accuracy. The position error vector can be formulated as:

$$\Delta_p^{est}(k) = p^h(k) - \hat{p}^h(k|k)$$

where $p^h(k)$ denotes the actual human position at time k.

Fig. 4 shows the position estimation error on longitudinal and lateral directions using four different estimators: Linear Kalman Filter (LKF), IMM-LKF, UKF and IMM-UKF. In the simulation, the same turn motion model in IMM-UKF is adopted for the system dynamics in UKF; the uniform motion model in IMM-LKF is also applied as the motion model in LKF. Several observations can be obtained in this figure. First, the responses of the nonlinear estimators such as UKF and IMM-UKF are faster than the linear estimators. Second, the IMM-based approaches show better performance in accuracy than the single-model approaches. Besides, IMM-UKF achieves the fastest response and best accuracy compared to other methods, especially when the human turns around the circular obstacle at time 50. Fig. 5 compares the velocity estimation using four estimators. Overall, the nonlinear estimators (UKF and IMM-UKF) show faster response compared to the linear estimators (LKF and IMM-LKF), though they have overshoots due to the fast response. It is worth noting that the overshoots of IMM-UKF are smaller than UKF while keeping the fast response at time 53 and 118 when the velocity changes abruptly. This makes sense as the IMM-UKF estimator incorporates uniform motion model that can capture the sudden velocity changes.

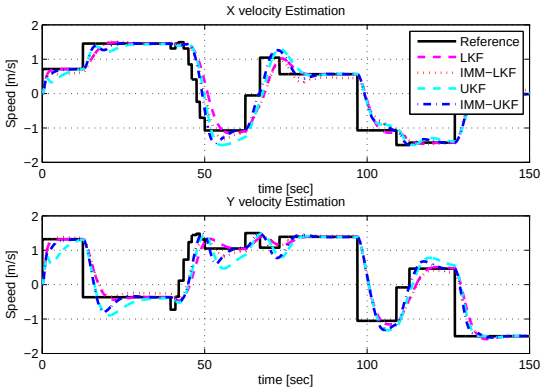

Fig. 5: Comparison of the estimated velocity using the IMM-based and the single-model approaches

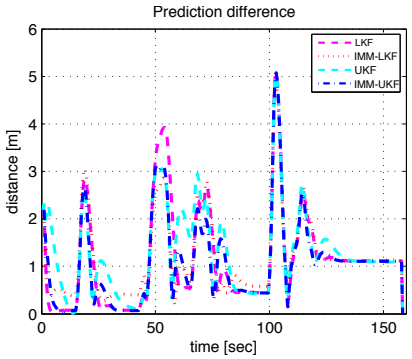

Fig. 6: Comparison of prediction error between the IMM-based and single-model approaches

2) Human motion prediction: To evaluate the IMM-UKF prediction, the average prediction error over the prediction horizon is computed and compared with the LKF, IMM-LKF and UKF. At time k, the prediction error is defined as:

$$\Delta_p^{pre}(k) = \frac{1}{N} \sum_{i=1}^{N} ||\tilde{p}^h(k+i|k) - p^h(k+i)||_2 \qquad (6)$$

Different from the IMM-based prediction approaches that extrapolate the human position by a weighted sum of the predicted positions from each model, the single-model methods only utilize one of the motion models for prediction.

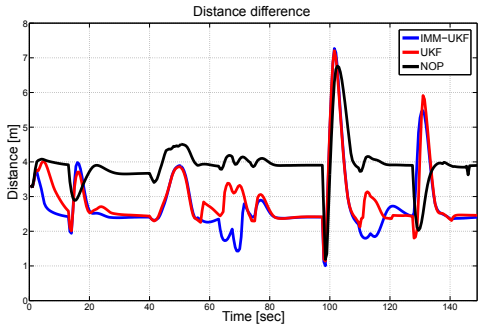

Fig. 7: Comparison of distance between the human and the robot using the MPC and the reactive methods

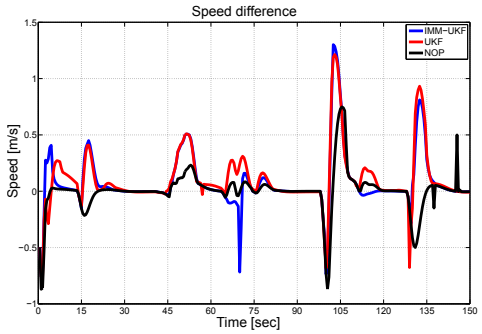

Fig. 8: Comparison of velocity difference between the human and the robot using the MPC and the reactive methods

Fig. 6 shows the comparison of prediction error using two single-model approaches (LKF, UKF) and two IMM-based methods (IMM-LKF, IMM-UKF). It can be noticed that single-model approaches generate larger prediction error than IMM-based methods, especially when the human makes turns, such as at time 50. This makes sense as IMM-based methods have already considered both uniform and turn motion models. Based on the simulation results, IMM-UKF is shown to outperform the other three prediction approaches.

3) Robot motion planning: Fig. 3d shows the trajectory of the companion robot that accompanies the target person moving in the field. The trajectory is generated by the proposed MPC motion planner with five-step planning horizon ($2.5s$) and using the IMM-UKF for predicting the human and moving obstacles' trajectories. The performance of the motion planning is evaluated using the criterion of safety and comfort. To be specific, the distance and speed differences between the robot and the human at each time step are measured, which are defined as:

$$\Delta_d(k) = ||p^r(k) - p^h(k)||_2 \tag{7a}$$

$$\Delta_v(k) = |v^r(k) - v^h(k)| \tag{7b}$$

The performance of IMM-UKF is compared with two benchmark prediction strategies, using the same MPC planner. The first benchmark method uses the coordinate turn motion model and applies UKF to predict human motion. The second method does not predict human motion. Instead, the robot only utilize the human's current state for one-step ($500ms$) motion planning.

Fig. 7 compares the distances between the human and the robot using these three strategies. It can be noticed that the MPC planner has ensured the safety of the accompanied human with each of the three prediction methods in that no distance goes below d_s. Additionally, by incorporating human motion prediction into the motion planning, the robot significantly improves its companion performance from the non-prediction case. In fact, the average distance between the human and the robot are 2.72, 2.88, 3.89 using the IMM-UKF, UKF and non-prediction methods respectively. Besides, the IMM-UKF achieves better performance than the UKF in that the average distance is smaller but still within the "comfort range" using the IMM-UKF.

The non-prediction method achieves smaller speed difference than methods using prediction, as shown in Fig. 8. This seems to imply that the non-prediction method is preferable for the robot in the sense of keeping similar pace as the human. However, it should be noted that such speed similarity leads to large distances between the human and the robot that are out of the 'comfort zone', as shown in Fig. 7, which is undesirable. In fact, the change of speed when using prediction results from the motion planner's effort to keep the robot within the comfort region around the human. Therefore, simulation results show the superiority of using the IMM-UKF prediction for robot motion planning.

V. CONCLUSION

We have developed an autonomous motion planning framework for human-companion robots to accompany a target person in a socially desirable manner. Such companion robot can be useful for search-and-rescue scenarios by assisting humans in carrying apparatus, exploring dangerous areas or detecting survivors. The IMM-UKF approach that incorporates the uniform motion model and the coordinated turn motion models is proposed for human motion estimation and prediction. Such multiple-model approach captures different human motion patterns, thus able to obtain accurate estimation and prediction. Based on the predicted human position and speed, a nonlinear programming is formulated using the model predictive control (MPC) approach for planning robot trajectory, which considers the safety and comfort of the robot behavior. Simulation results show superior performance in terms of the accuracy and response time in the estimation and prediction using the IMM-UKF approach compared to other three approaches: LKF, IMM-LKF and UKF, especially when the human makes curved motion or sharp turns. Moreover, the MPC planner is evaluated using the IMM-UKF, the UKF and non-prediction methods. The planner successfully ensures the safety of the accompanied person using all these prediction strategies. The IMM-UKF results in best robot motion behavior by keeping the robot closest to the comfort distance from the human.

In the future work, we plan to compare other motion prediction methods, such as the auto-regressive moving-average (ARMA) method, with IMM-UKF method. Besides, enabling the robot to learn human motion model in real time is an attractive topic and may provide more accurate human motion prediction and results in better human-companion behavior.

APPENDIX

A. IMM-LKF Method

Similar to IMM-UKF, IMM-LKF works with two motion models: the uniform motion model and the coordinated turn motion model. If the turn rate is a known constant in the coordinated turn motion model, the human estimation procedure can be modeled with the discrete time linear system as follows:

$$x^h(k+1) = Ax^h(k) + B_w w(k) \tag{8a}$$

$$y^h(k) = Cx^h(k) + v(k) \tag{8b}$$

where $x^h(k)$ and $y^h(k)$ represent the human motion state and the observation, respectively, at the time step k; $w(k)$ and $v(k)$ represent process noise and measurement noise, respectively. $x^h(k)$ consists of four elements: $p_1^h, v_1^h, p_2^h, v_2^h$, where p_1^h, p_2^h denote the longitudinal and lateral position of the human and v_1^h, v_2^h the corresponding velocity. We use two LKFs in the IMM for human tracking, each corresponding to a different kinematic model: the uniform motion model and the turn motion model. Two models differ in the A matrix and w in Eq. (8a) while sharing the same B_w. In particular, we define the matrices as follows:

$$A_U = \begin{bmatrix} 1 & T & 0 & 0 \\ 0 & 1 & 0 & 0 \\ 0 & 0 & 1 & T \\ 0 & 0 & 0 & 1 \end{bmatrix}, A_T = \begin{bmatrix} 1 & \frac{\sin(\omega T)}{\omega} & 0 & \frac{1-\cos(\omega T)}{\omega} \\ 0 & \cos(\omega T) & 0 & -\sin(\omega T) \\ 0 & \frac{1-\cos(\omega T)}{\omega} & 1 & \frac{\sin(\omega T)}{\omega} \\ 0 & \sin(\omega T) & 0 & \cos(\omega T) \end{bmatrix}$$

$$B_w = \begin{bmatrix} \frac{T^2}{2} & T & 0 & 0 \\ 0 & 0 & \frac{T^2}{2} & T \end{bmatrix}, w_U \sim \mathcal{N}(0, Q_U),\ w_T \sim \mathcal{N}(0, Q_T)$$

where A_U and A_T stand for the A matrices of the uniform motion model and turn motion model, respectively; w_U and w_T denote the process noise of the uniform motion model and turn motion model, respectively; T represents the sampling time; ω represents the constant turn rate.

We assume that only the human position can be measured. Therefore, the parameters in observation model Eq. (8b) can be defined as:

$$C = \begin{bmatrix} 1 & 0 & 0 & 0 \\ 0 & 0 & 1 & 0 \end{bmatrix}, v \sim \mathcal{N}(0, V)$$

Moreover, we set the turn rate ω to be 0.1 rad/s as a known constant, in the turn motion model in IMM-LKF.

B. Approximating Static Obstacles

Static rectangular obstacles are approximated and analytically represented as ellipses, as shown in Fig. 9. Let a and b be the length and width of a rectangular obstacle centered at the origin. Let Eq. (9) represent the ellipse that encloses the obstacle in the way that the four vertices of the rectangle lie on the boundary of the ellipse:

$$\frac{x^2}{\alpha^2} + \frac{y^2}{\beta^2} = 1 \tag{9}$$

In addition, assume that the rectangle and ellipse have the same aspect ratio, which means $\frac{a}{b} = \frac{\alpha}{\beta}$, then by simple algebraic manipulation, we can obtain that $\alpha = \frac{a}{\sqrt{2}}$ and $\beta = \frac{b}{\sqrt{2}}$. Define $h(x,y) = 2\frac{x^2}{a^2} + 2\frac{y^2}{b^2} - 1$. Then $h(x,y) = 0$ represent the ellipse approximation of the rectangle with length a and width b. Any point (x,y) with $h(x,y) > 0$ lies outside of the ellipse.

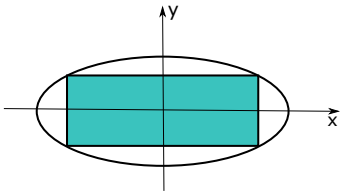

Fig. 9: Approximating the rectangle obstacle with an ellipse.

REFERENCES

[1] J. Casper and R. R. Murphy, "Human-robot interactions during the robot-assisted urban search and rescue response at the world trade center," *Systems, Man, and Cybernetics, Part B: Cybernetics, IEEE Transactions on*, vol. 33, no. 3, pp. 367–385, 2003.

[2] I. R. Nourbakhsh, K. Sycara, M. Koes, M. Yong, M. Lewis, and S. Burion, "Human-robot teaming for search and rescue," *Pervasive Computing, IEEE*, vol. 4, no. 1, pp. 72–79, 2005.

[3] G.-J. M. Kruijff, F. Colas, T. Svoboda, J. Van Diggelen, P. Balmer, F. Pirri, and R. Worst, "Designing intelligent robots for human-robot teaming in urban search and rescue.," in *AAAI Spring Symposium: Designing Intelligent Robots*, 2012.

[4] T. Kruse, A. K. Pandey, R. Alami, and A. Kirsch, "Human-aware robot navigation: A survey," *Robotics and Autonomous Systems*, vol. 61, no. 12, pp. 1726–1743, 2013.

[5] M. Svenstrup, T. Bak, and H. J. Andersen, "Trajectory planning for robots in dynamic human environments," in *Intelligent Robots and Systems (IROS), 2010 IEEE/RSJ International Conference on*, pp. 4293–4298, IEEE, 2010.

[6] E. T. Hall, R. L. Birdwhistell, B. Bock, P. Bohannan, A. R. Diebold Jr, M. Durbin, M. S. Edmonson, J. Fischer, D. Hymes, S. T. Kimball, *et al.*, "Proxemics [and comments and replies]," *Current anthropology*, pp. 83–108, 1968.

[7] M.-L. Barnaud, N. Morgado, R. Palluel-Germain, J. Diard, and A. Spalanzani, "Proxemics models for human-aware navigation in robotics: Grounding interaction and personal space models in experimental data from psychology," in *Proceedings of the 3rd IROS2014 workshop Assistance and Service Robotics in a Human Environment*, 2014.

[8] P. Henry, C. Vollmer, B. Ferris, and D. Fox, "Learning to navigate through crowded environments," in *Robotics and Automation (ICRA), 2010 IEEE International Conference on*, pp. 981–986, IEEE, 2010.

[9] D. Koller, J. Weber, and J. Malik, *Robust multiple car tracking with occlusion reasoning*. Springer, 1994.

[10] Y. Rui and Y. Chen, "Better proposal distributions: Object tracking using unscented particle filter," in *Computer Vision and Pattern Recognition, 2001. CVPR 2001. Proceedings of the 2001 IEEE Computer Society Conference on*, vol. 2, pp. II–786, IEEE, 2001.

[11] M. Bennewitz, W. Burgard, G. Cielniak, and S. Thrun, "Learning motion patterns of people for compliant robot motion," *The International Journal of Robotics Research*, vol. 24, no. 1, pp. 31–48, 2005.

[12] C. Fulgenzi, C. Tay, A. Spalanzani, and C. Laugier, "Probabilistic navigation in dynamic environment using rapidly-exploring random trees and gaussian processes," in *Intelligent Robots and Systems, 2008. IROS 2008. IEEE/RSJ International Conference on*, pp. 1056–1062, IEEE, 2008.

[13] J. K. Aggarwal and Q. Cai, "Human motion analysis: A review," *Computer vision and image understanding*, vol. 73, no. 3, pp. 428–440, 1999.

[14] B.-S. Yaakov, X. Li, and K. Thiagalingam, "Estimation with applications to tracking and navigation," *New York: Johh Wiley and Sons*, vol. 245, 2001.

[15] D. S. Caveney, "Multiple model techniques in automotive estimation and control," tech. rep., 2004.

[16] S. Haykin, *Kalman filtering and neural networks*, vol. 47. John Wiley & Sons, 2004.

[17] S. Hong, T. Smith, F. Borrelli, and J. K. Hedrick, "Vehicle inertial parameter identification using extended and unscented kalman filters," in *Intelligent Transportation Systems-(ITSC), 2013 16th International IEEE Conference on*, pp. 1436–1441, IEEE, 2013.